

Supplementary Information for

Conformational ensembles of neuromedin C reveal a progressive coil-helix transition within a binding-induced folding mechanism

Miquel Adrover^{*a,b}, Pilar Sanchis^{a,b}, Bartolomé Vilanova^{a,b}, Kris Pauwels^{c,d}, Gabriel Martorell^e and Juan Jesús Pérez^f

^aInstitut Universitari d'Investigació en Ciències de la Salut (IUNICS). Departament de Química, Universitat de les Illes Balears, Ctra. Valldemossa km 7.5, E-07122 Palma de Mallorca, Spain.

^bInstituto de Investigación Sanitaria de Palma (IDISPA), Ctra. Valldemossa, 79, E-07010, Palma de Mallorca, Spain.

^cStructural Biology Brussels, Vrije Universiteit Brussels, Pleinlaan 2, 1050 Brussels, Belgium.

^dVIB Structural Biology Research Centre, Vlaams Instituut voor Biotechnologie, Pleinlaan 2, 1050 Brussels, Belgium.

^eServeis Científico-Tècnics, Universitat de les Illes Balears, Ctra. Valldemossa km 7.5, E-07122 Palma de Mallorca, Spain.

^fDepartament d'Enginyeria Química, Universitat Politècnica de Catalunya, ETSEIB, Av. Diagonal, 647; E-08028 Barcelona, Spain

*Correspondence to: Miquel Adrover, University of Balearic Islands,
Phone: 0034 971 173491; Fax 0034 971 1732;
e-mail: miquel.adrover@uib.es

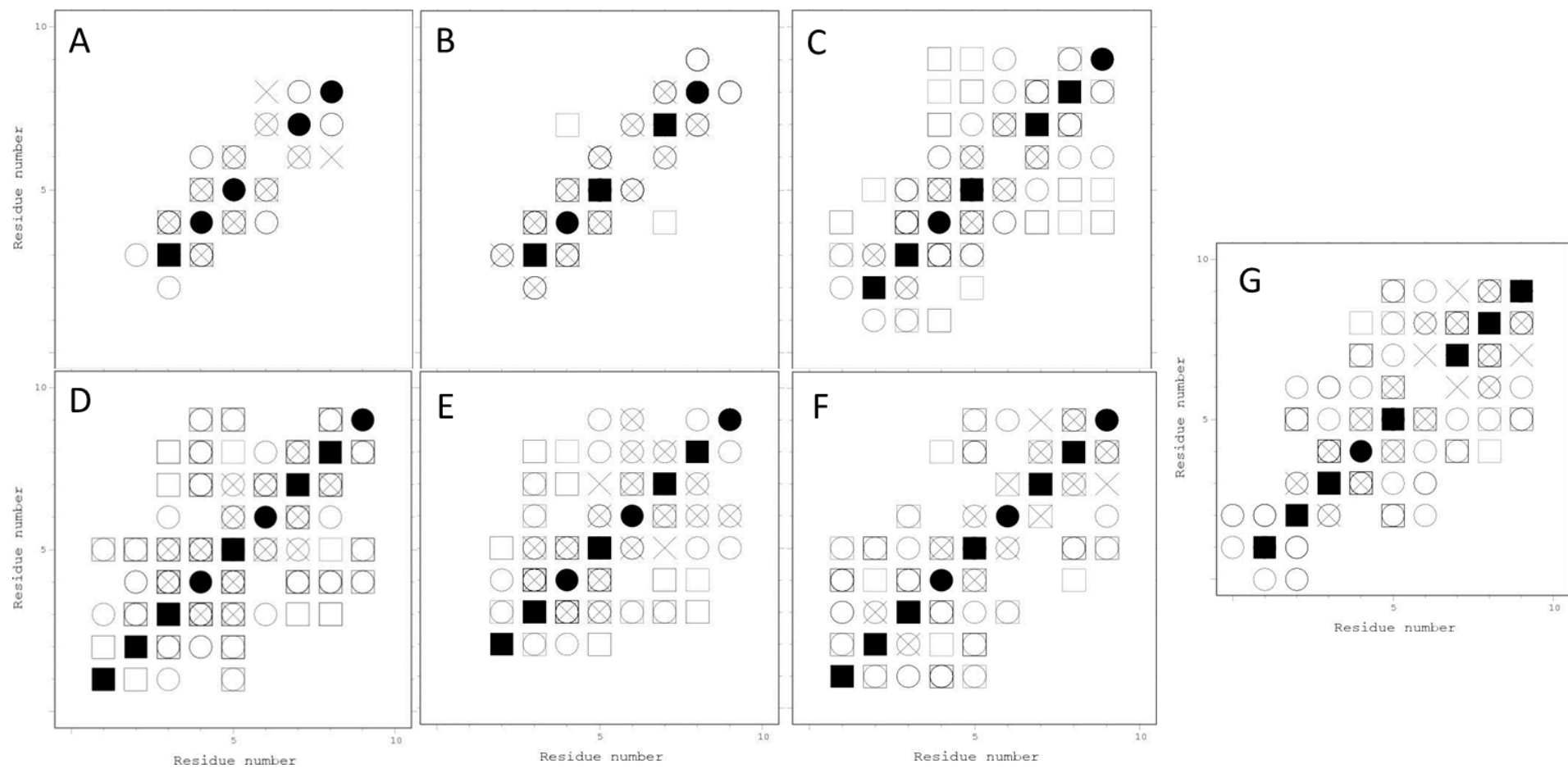


Figure S1. Contact maps for NMC structures calculated in the presence of (A) 0%, (B) 10%, (C) 25%, (D) 40%, (E) 60% and (F) 90% d₃-TFE, and in the presence of (G) 150mM d₂₅-SDS. The geometrical restraints yielding these contact maps were taken from the ¹H,¹H NOEs intensities using an automatic assignment process. X represents backbone-backbone interactions; \blacksquare represents backbone-side chain interactions (filled if intraresidue); \square represents side chain-side chain interactions (filled if intraresidue). The contact maps plots were obtained analyzing the solution structure through the Protein Structure Validation Server (PSV) (http://psvs-1_4-dev.nesg.org/).⁶⁹

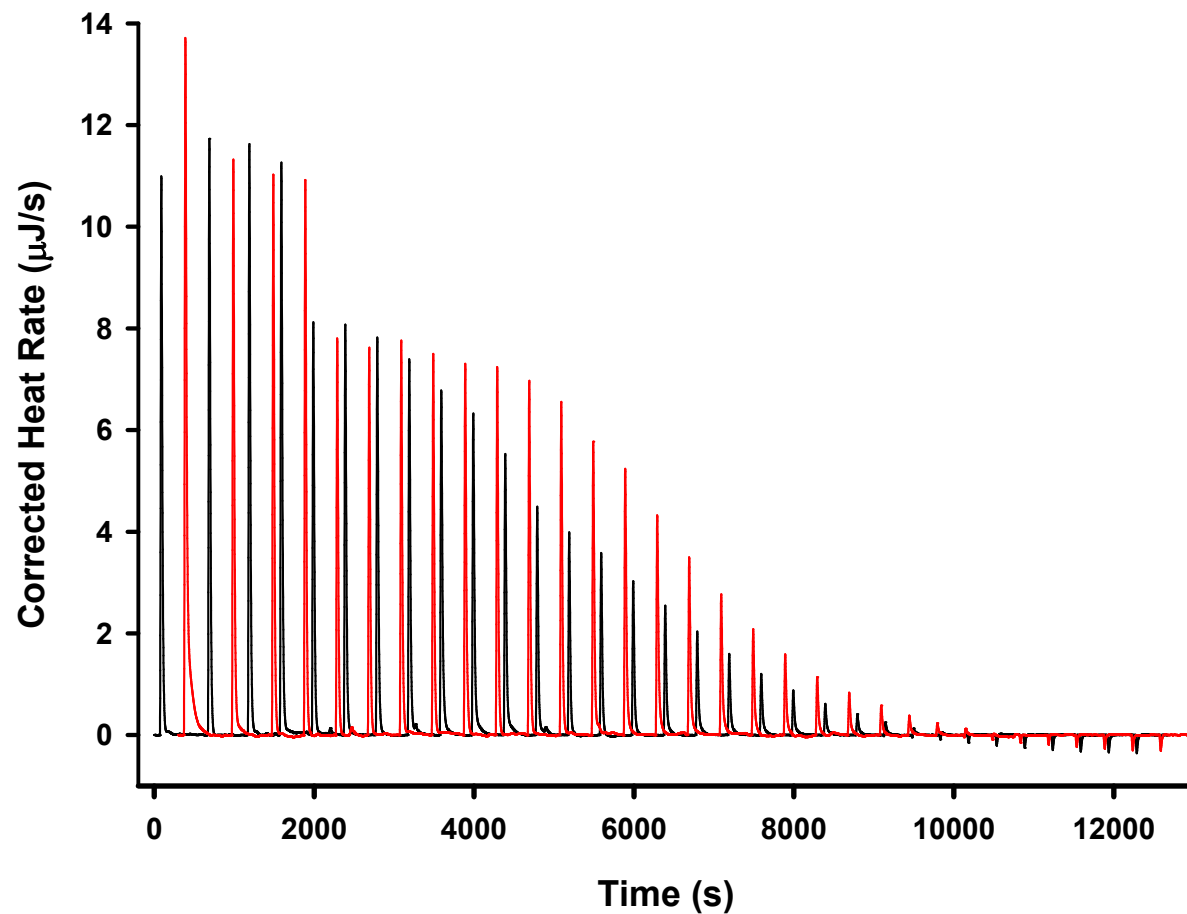


Figure S2. Heat flow versus time profiles resulting from injection of $2\mu\text{l}$ (the first four injections) or $1.5\mu\text{l}$ (the other injections) aliquots of a 10mM acetate buffered solution (pH 4.0) of SDS at 35mM concentration into a $171\mu\text{l}$ reaction cell containing a 10mM acetate buffer solution either alone (*black*) or in presence of $42\mu\text{M}$ of NMC (*red*). The titration plot representing the experiment carried out on NMC has been shifted on the graph 300s towards higher injection times to have a better comparison between both plots.

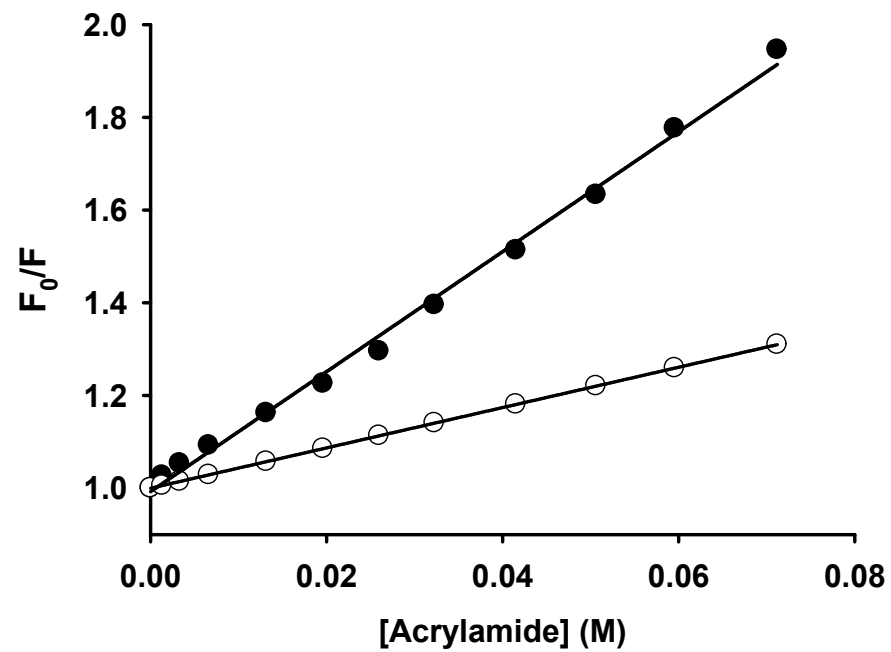


Figure S3. Stern-Volmer plots for the quenching of a 0.1mM NMC buffered solution solution alone (●) and in presence of 50mM SDS (□). F and F_0 are the fluorescence intensities in the presence and absence of acrylamide, respectively (λ_{exc} 280nm; λ_{em} 356nm in ● and λ_{em} 345nm in □).

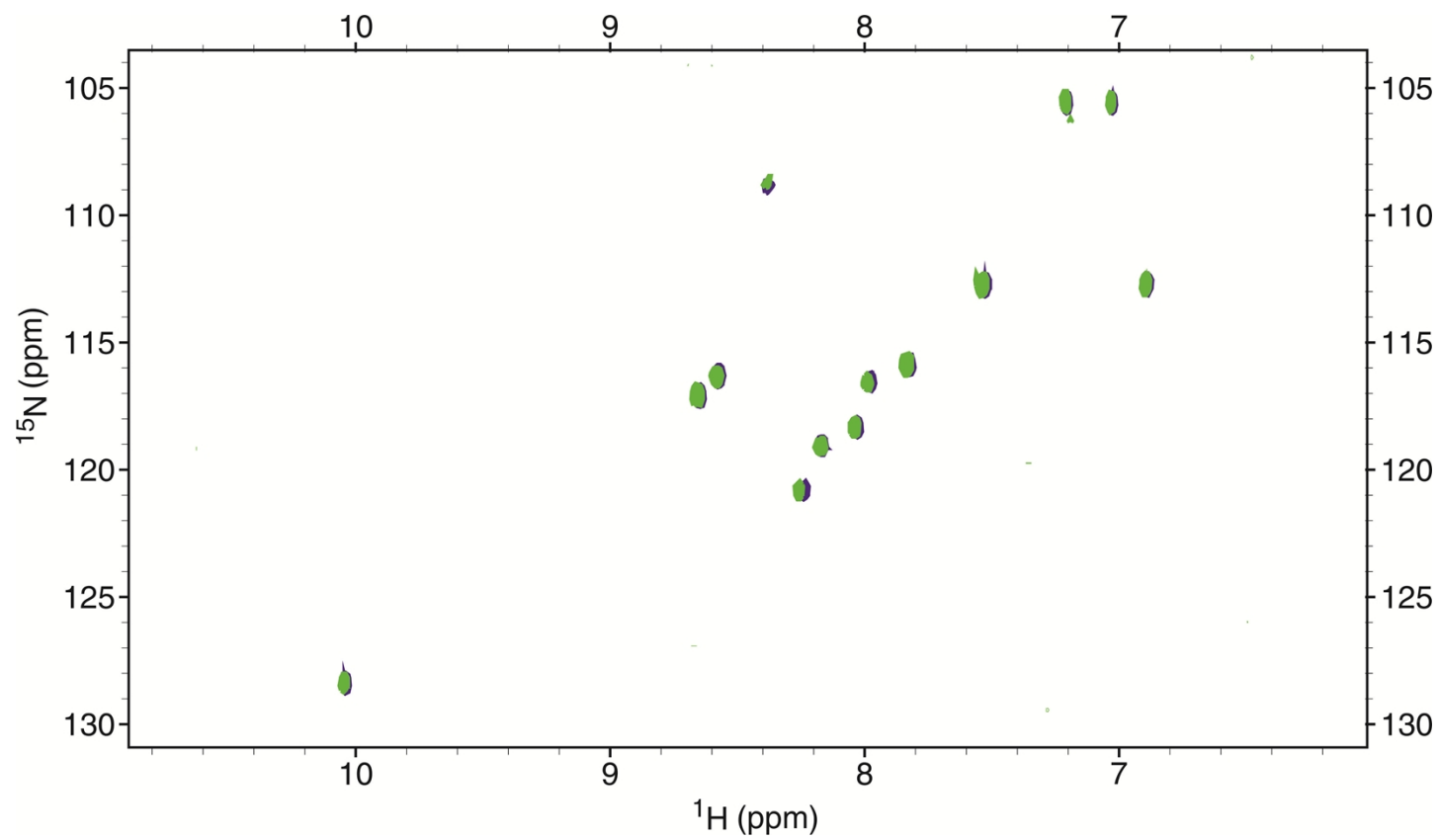


Figure S4. Overlapping of the ^{15}N -HSQC spectra of NMC recorded at 15°C in 10mM acetate buffer (pH 4.0) in presence of 150mM $\text{d}_2\text{-SDS}$ (*blue*) and in presence of 50mM SDS (*green*).

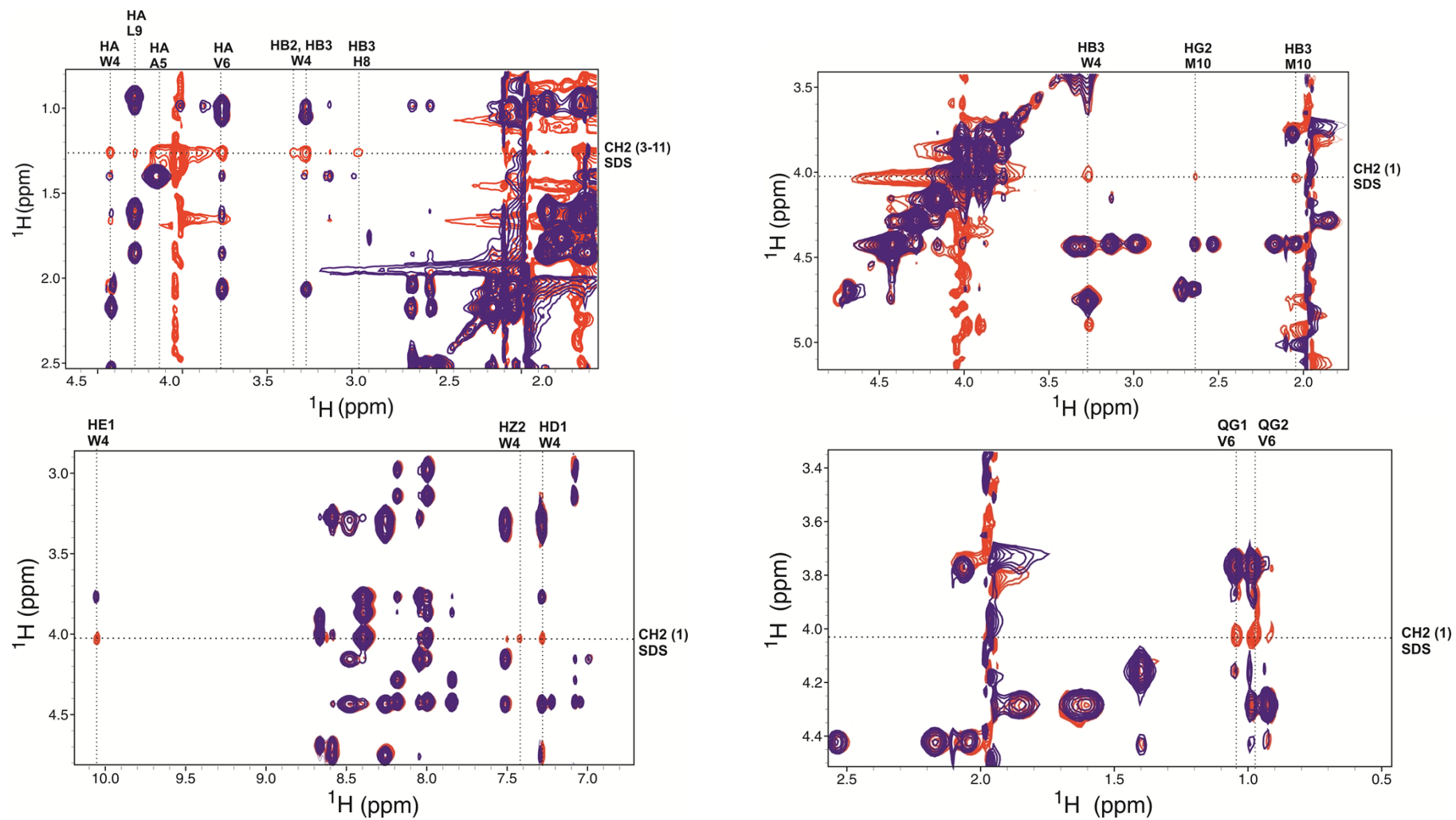


Figure S5. Overlap of the ^1H , ^1H -NOESY spectra of NMC at different spectral regions when NMC was bound to SDS micelles (*red*) and when it was bound to d_{25} -SDS micelles (*blue*).

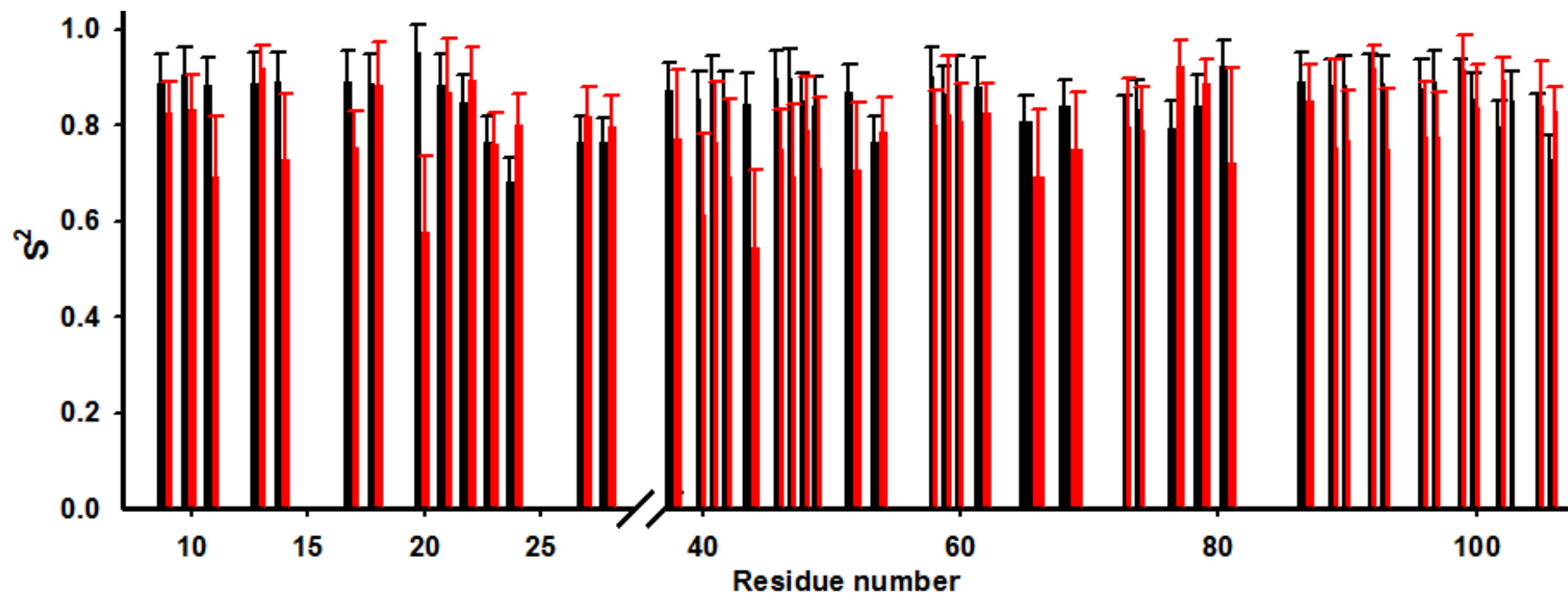


Figure S6. Generalized order parameters (S^2) of CyaY in 25mM Tris-HCl buffer at pH 8.3 (*black bars*) and in hen egg white (*red bars*) as a function of the residue number. S^2 values were calculated using previously published R_1 , R_2 and HET-NOE data⁵⁹ by applying the Liparizi-Szabo model-free analysis.

Table S1. Secondary structure contents of NMC at different TFE percentages estimated from the corresponding CD spectrum acquired in 10mM acetate buffer (pH 4.0) at 15°C.

% TFE	% Helix^a	% Antiparallel β-sheet^a	% Turns^a	% Random Coil^a
0	3.4	35.6	10.7	50.3
10	3.8	33.8	12	50.4
25	10.6	29.6	11.2	48.6
40	26.8	21.8	7.0	44.7
60	37.3	17.1	3.9	41.8
90	44.3	10.9	7.2	37.6
SDS	36.8	23.2	0.0	40.0

^a The secondary structure contents were estimated by using the BeStSel on-line platform (<http://bestsel.elte.hu/>)

Table S2. Residue-specific dynamics parameters calculated from the Lipari-Szabo model-free formalism at 14.1T for NMC in 10mM acetate buffer at pH 4.0 and 15°C.

Residue	Model	χ^2	S^2	τ_e , ps
2	2	2.76	0.23±0.03	80±16
3	2	0.19	0.37±0.03	173±31
4	2	0.055	0.47±0.02	137±22
5	2	0.082	0.62±0.01	22±7
6	2	0.117	0.48±0.02	80±9
7	2	0.054	0.54±0.01	82±10
8	2	0.178	0.53±0.02	50±9
9	2	0.093	0.41±0.02	60±7
10	2	0.651	0.37±0.02	140±15

Table S3. Residue-specific dynamics parameters calculated from the Lipari-Szabo model-free formalism at 14.1T and 15°C for a NMC solution containing 60% TFE and 40% acetate buffer (10mM) at pH 4.0.

Residue	Model	χ^2	S^2	τ_e , ps	R_{ex} , s ⁻¹	S_f^2 ^a
3	4	0.14	0.68±0.15	510±110	3.65±0.67	-
4	2	0.31	0.74±0.01	112±15	-	-
5	2	0.83	0.79±0.02	71±16	-	-
6	2	1.58	0.68±0.01	98±12	-	-
7	2	2.85	0.75±0.01	59±12	-	-
8	2	0.006	0.75±0.02	99±17	-	-
9	5	0.000	0.43±0.10	1190±322	-	0.89±0.02
10	5	0.000	0.42±0.06	694±167	-	0.85±0.02
^a $S^2 = S_f^2 \cdot S_s^2$						

Table S4. Residue-specific dynamics parameters calculated from the Lipari-Szabo model-free formalism at 14.1T for NMC under its SDS micelle bound state, at pH 4.0 and 15°C.

Residue	Model	χ^2	S^2	τ_c , ps	R_{ex} , s ⁻¹	S_f^2 ^a
2	5	0.00	0.43±0.06	743±173	-	0.79±0.07
3	1	3.90	0.84±0.04	-	-	-
4	1	4.40	0.86±0.07	-	-	-
5	4	0.00	0.64±0.06	64±35	6.0±2.6	-
6	1	5.00	0.87±0.06	-	-	-
7	1	3.50	0.86±0.07	-	-	-
8	3	3.11	0.93±0.07	-	2.1±0.9	-
9	1	0.82	0.79±0.06	-	-	-
10	2	0.00	0.77±0.02	597±356	-	-
^a $S^2 = S_f^2 \cdot S_s^2$						